ELSEVIER

Polymer 43 (2002) 477–487

polymer

www.elsevier.com/locate/polymer

Projection from an atomistic chain contour to its primitive path ☆

Martin Kröger[a,b,*], Jorge Ramírez[a,c], Hans Christian Öttinger[a]

[a]*Department of Materials, Institute of Polymers, ETH Zentrum, CH-8092 Zurich, Switzerland*
[b]*Institut für Theoretische Physik, Technische Universität Berlin, D-10623 Berlin, Germany*
[c]*Department of Chemical Engineering, Laboratory of Non-Metallic Materials, ETSII/UPM, Jose Gutierrez Abascal 2, E-28006 Madrid, Spain*

Abstract

In this note, we propose a mapping from the spatial coordinates of an atomistic polymer chain to its 'primitive path' (PP), a concept being frequently used in the framework of reptation models. For the model to be presented, the projection preserves as much structure of the atomistic chain as appropriate to replace an atomistic chain on a prescribed (parameterized) coarse-grained level. We present an efficient numerical method to extract a PP as well as an analytic approach to study the conformational properties of the coarse-grained chain in an approximate fashion. The knowledge of the PP is a prerequisite to facilitate tests of mesoscopic descriptions of polymeric fluids, in particular in the framework of nonequilibrium thermodynamics, and allows for a thorough analysis of atomistic chain configurations on a 'relevant' coarse-grained level.

Keywords: Polymer; Primitive path; Coarse-graining

1. Introduction

There have been many attempts to understand the behavior of atomistic model fluids by defining and investigating conformational quantities, which aim to characterize the atomistic system on a coarse-grained level. The most prominent goal is to setup (projection) operators which act on the space coordinates of atoms such that the resulting quantities serve either as slow variables needed to proceed with a separation of time scales in the corresponding Langevin equations, or to characterize the system by structural quantities, which are known to be within reach of analytical theoretical descriptions or/and accessible by experiments.

For example, in Ref. [1] Lee and Mattice presented an alternative way — beyond grid techniques — of looking at the *static free volume* in atomistic simulations, where the atoms are represented by hard spheres. They defined phantom bubbles (empty spheres), which contact four or more hard spheres of atoms simultaneously in three-dimensional space and do not overlap with any atom in the structure. Using this procedure, and by studying the morphology of the voids, they presented a new basis to establish an alternative relationship between simulation and experiments. Their procedure reduces the number of degrees of freedom needed to describe the state of the system. An attempt has been made to characterize the *degree of entanglement* in linear polymeric model systems, based on the mutual overlap of static secant volumes for pairs of chains in Refs. [2,3]. Different measures of geometrical entanglement information, such as algebraic description via knot polynomials, differential geometric approaches, path integral approaches via Abelian and non-Abelian Chern–Simons field theory, have been extensively discussed and compared to each other in Ref. [4].

Here, we will be concerned with two other 'coarse-grained' quantities which entered the theoretical description of the dynamics of polymers in 1978, the PP and the 'tube' introduced by Doi and Edwards [5,6]. There has been no definition stated based on the atomistic coordinates of a given model system, although the concept is widely accepted and turned out to be useful in many aspects [7]. For example, the problem of the 'primitive path' (PP) statistics of an entangled lattice polymer has been mapped into the simple problem of a biased one-dimensional random walk with reflecting barrier at one end in Refs. [8,9]. Definitions for these quantities should enable the study of the transient behavior of PPs and tubes in order to compare analytic model predictions with the 'true dynamics' obtained by computer experiments. Another motivation stems from canonical ensemble atomistic simulations for

☆ This paper was originally submitted to *Computational and Theoretical Polymer Science* and received on 22 November 2000; received in revised form on 22 February 2001; accepted on 25 February 2001. Following the incorporation of *Computational and Theoretical Polymer Science* into *Polymer*, this paper was consequently accepted for publication in *Polymer*.

* Corresponding author. Address: Department of Materials, Institute of Polymers, ETF Zentrum, CH-8092 Zurich, Switzerland. Fax: +41-1-632-1076.

E-mail address: mkroeger@ifp.mat.ethz.ch (M. Kröger).

0032-3861/02/$ - see front matter
PII: S0032-3861(01)00422-0

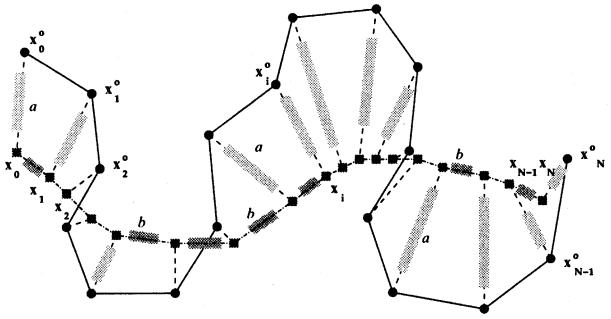

Fig. 1. The projection results from minimization of the energy of the depicted mechanical system and contains a single parameter $\zeta = b/a$, the ratio of spring coefficients. Black dots: atomistic chain, squares: beads of the PP.

linear polymers in nonequilibrium flow situations, recently established in Ref. [10]. Besides conventional variables entering the control (accept/reject) scheme of a Monte Carlo simulation, a number of *structural variables* (based on atomistic coordinates, such as alignment or single conformation tensors [11] or multiple conformation tensors) have been taken into account. While Ref. [10] set the framework for designing realistic atomistic Monte Carlo simulations by referring to thermodynamically admissible macroscopic models derived from the 'general equation for the nonequilibrium reversible–irreversible coupling' (GENERIC) [12,13], no definitions have been developed for the desired sophisticated projections from atomistic to coarse-grained variables to be used for the implementation of the PP idea. A possible simple procedure will be outlined in this article which also fulfils two relevant criteria for applications: (i) it has maximum efficiency, i.e. the procedure is linear in the number of particles and (ii) it allows for an analytical treatment due to its mechanical analog. In order to establish the 'projection' we will analyze and visualize its features for most simple cases such as the freely jointed atomistic chain (FJC).

2. Discrete version of the primitive path

The definition of the PP given by Doi and Edwards [14] states that it must be the shortest path connecting the two ends of the chain with the same topology as the chain itself relative to the obstacles. From this definition it can be extracted that the path must be a line following the contour of the chain but in a softer way, avoiding all the kinks that the chain might have. This idea is now used to define a corresponding projection.

The desired mapping $\mathscr{P}$, parameterized by a single parameter ζ, $\mathscr{P}_\zeta : \{\mathbf{x}_i^o\} \rightarrow \{\mathbf{x}_i\}$ maps a set of $i = 0, 1, \ldots, N$ atomistic coordinates $\mathbf{x}_i^o$ of a linear discrete chain (in d dimensions for convenience) to a new set with an equal number of coordinates, called coarse-grained coordinates $\mathbf{x}_i$, which define the coarse-grained chain or PP $\{\mathbf{x}_i\}$ of the atomistic chain. We require, that $\mathscr{P}_0 = Id$, i.e. for $\zeta = 0$ all information of the atomistic chains is conserved for the coarse-grained chain. The opposite limit must reflect a complete loss of information about the atomistic structure, i.e the projection in the limit $\zeta \rightarrow \infty$ should give a straight line (or point) for arbitrary atomistic configurations. In addition, for physical reasons the projection should at least approximately conserve the center of mass, it should possess head-tail symmetry and we require that the persistence (flexibility) length of the coarse-grained chain varies monotonically with the parameter ζ. These conditions leave a limited number of qualitatively different possibilities. We now propose a projection that fulfills these criteria. It is defined as the solution of minimization of the energy

$$E \propto \frac{1}{2}\sum_{i=0}^{N}(\mathbf{x}_i - \mathbf{x}_i^o)^2 + \frac{\zeta^2}{2}\sum_{i=0}^{N-1}(\mathbf{x}_{i+1} - \mathbf{x}_i)^2, \tag{1}$$

for a mechanical system of two types of Hookean springs, as depicted in Fig. 1. The first type connects adjacent beads within the (projected) PP, the second type connects the (projected) beads of the PP with the atomistic (original) beads, in order to achieve $\mathscr{P}_0 = Id$. The coordinates of the PP are obtained by solving the force equations $\partial E/\partial \mathbf{x}_i = 0$. The result reads

$$(\mathbf{x}_i - \mathbf{x}_i^o) - \zeta^2(\mathbf{l}_{i+1} - \mathbf{l}_i) = 0 \qquad \text{for } i \in 0, \ldots, N, \tag{2}$$

where we have introduced the connector between neighbors along the chains contour $\mathbf{l}_i \equiv \mathbf{x}_i - \mathbf{x}_{i-1}$ for $i \in 1, \ldots, N$, and $\mathbf{l}_0 = \mathbf{l}_{N+1} \equiv 0$ in order to keep notation short. Eq. (2) can be rewritten as $\mathbf{x} = \mathscr{P}' \cdot \mathbf{x}^o$, where we have collected all coordinates $\mathbf{x}_i$ (same for $\mathbf{x}_i^o$) into a single dN-dimensional vector $\mathbf{x} = (\mathbf{x}_0, \mathbf{x}_1, \ldots, \mathbf{x}_N)^T$ and $\mathscr{P}$ is the quadratic $(N+1)\times(N+1)$ projection matrix. Our model explicitly provides the inverse projection matrix $\mathscr{P}^{-1}$

$$\mathscr{P}^{-1} = \begin{pmatrix} 1+\zeta^2 & -\zeta^2 & 0 & \cdots & \cdots & 0 \\ -\zeta^2 & 1+2\zeta^2 & -\zeta^2 & 0 & \ddots & \vdots \\ 0 & -\zeta^2 & 1+2\zeta^2 & \ddots & \ddots & \vdots \\ \vdots & \ddots & \ddots & \ddots & -\zeta^2 & 0 \\ \vdots & \ddots & 0 & -\zeta^2 & 1+2\zeta^2 & -\zeta^2 \\ 0 & \cdots & \cdots & 0 & -\zeta^2 & 1+\zeta^2 \end{pmatrix} \tag{3}$$

possessing a tridiagonal structure and thus, can be inverted in $O(N^1)$ operations, see, e.g. Ref. [15]. 'Coarse-graining' itself is achieved, and information about atomistic details is virtually lost with increasing parameter ζ. Summation over i in Eq. (2) yields one of the desired properties of the projection, the conservation of center of mass, i.e. $\sum_{i=0}^{N}\mathbf{x}_i = \sum_{i=0}^{N}\mathbf{x}_i^o$. Other quantities, such as the contour length $L = \sum_i |\mathbf{l}_i|$ are sensitive to ζ. This is most easily shown by considering a continuous analog, but since the projection,

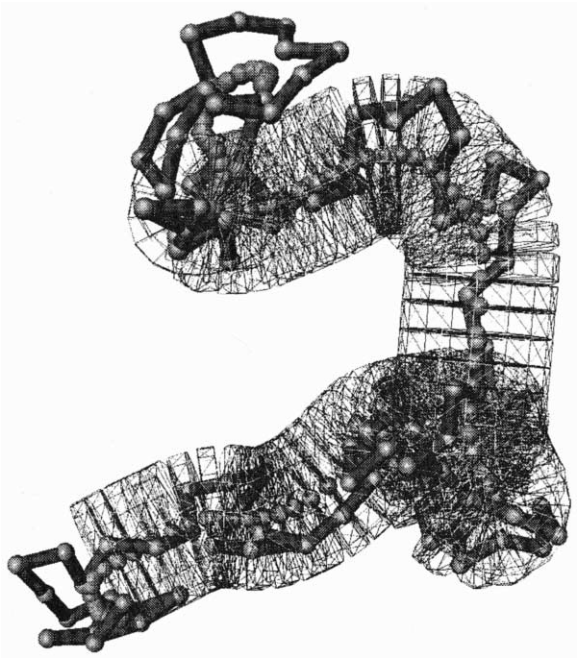

Fig. 2. The contour of: (i) an atomistic chain — fluctuating path, grey beads, black segments — and (ii) its PP — the smooth path, grey beads, no segments visible — constructed from the atomistic chain with the same number of beads ($N = 140$). The surrounding cylinders are aligned in direction of the PP (for $\zeta = 5$).

as indirectly defined already through Eq. (2) is explicitly needed to devise an efficient algorithm, we will keep on discussing the discrete projection first. A PP resulting from the described operation is depicted in Fig. 2. The parameter ζ of the projection may be interpreted in various ways. As will be seen below, ζ controls the Kuhn's length b_K (twice the persistence length l_p), contour length L and 'width' of the PP, or 'tube diameter'. If the relevant model parameter should be the number of Kuhn's elements Z (or 'entanglements' with respect to the picture of Doi and Edwards), we have $Z = Nb_0^2/b_K^2$, where b_0^2 denotes the mean squared atomistic bond length. Also the contour length L or tube diameter may be regarded as alternative system parameters, depending on anticipated interpretation.

The speed required for an inversion of $\mathscr{P}^{-1}$ in Eq. (3) is, e.g. for $N < 10^5$, some orders of magnitude faster than a typical Monte Carlo step — even when assumed to scale with $O(N^0)$ — and thus it turns out to be unproblematic to perform the projection often enough in order to analyze dynamical properties, or correlations. It is evident, that the speed of inversion is unaltered if we introduce functions $\zeta = \zeta(i)$, but it will become a time consuming operation if we consider non-Hookean springs or additional forces such as a Maxwell Daemon pulling at the ends of the PP (in order to preserve a certain tension in the primitive chain; see also discussion in Section 6.2).

For the sake of completeness, we also note the resulting explicit connection between segment vectors before and after the transformation, viz.

$$\mathbf{l}_i = A_{ij}^{-1}\mathbf{l}_i^0, \tag{4}$$

with $A_{ij} \equiv (1 + 2\zeta^2)\delta_{ij} - \zeta^2(\delta_{i,j+1} + \delta_{i,j-1})$ ($\mathbf{A}$ has dimension $N \times N$) as well as the expression for the $N + 1$ vectors $\mathbf{Q}_i$ connected with the a-springs in Fig. 1, which we should call 'tube vectors' in the following:

$$\mathbf{Q}_i \equiv \mathbf{x}_i - \mathbf{x}_i^o = \sum_{j=1}^{N} D_{ij}\mathbf{l}_j, \tag{5}$$

where $D_{ij} \equiv \zeta^2(\delta_{ij} - \delta_{i,j+1})$ ($\mathbf{D}$ has dimension $(N + 1) \times N$).

3. Continuous version of the PP

In order to derive some properties of the stated projection $\mathscr{P}$, in particular the effect of ζ on the persistence length of the coarse-grained chain, we reformulate the projection in terms of a differential equation plus boundary conditions. Both descriptions become equivalent in the long chain limit (exactly, for constant $|\mathbf{l}_i^o|$ for all i). We let the discrete chain approximate a continuous line with fixed contour length L by labeling the discrete chain with a continuous dimensionless label $s = [0, 1]$; neighboring atoms at contour position $s_i = i\Delta s$ are now separated by $\Delta s = 1/N$. With these definitions the mechanical energy (1) reads in the continuous limit

$$E \propto \int_0^1 [(\mathbf{x}(s) - \mathbf{x}^o(s))^2 + \zeta_c^2|\mathbf{x}'(s)|^2]\,\mathrm{d}s, \tag{6}$$

where one notices, that the quantity $\zeta_c \equiv \zeta/N$ turns out to determine the overall shape of the continuous chain and is therefore to be regarded as the intrinsic parameter of the projection, i.e. if we double the number of beads on a given atomistic contour, we will obtain a comparable shape of the coarse-grained chain if we keep ζ_c, but not ζ, fixed. The functional (6) is minimized by solving the corresponding Euler–Lagrange differential equation

$$\zeta_c^2\mathbf{x}''(s) - \mathbf{x}(s) = -\mathbf{x}^o(s). \tag{7}$$

Two boundary conditions can be extracted from the continuous limit of Eq. (2): $\mathbf{x}(0) - \mathbf{x}^o(0) - N\zeta_c^2\mathbf{x}'(0) = 0$ and $\mathbf{x}(1) - \mathbf{x}^o(1) + N\zeta_c^2\mathbf{x}'(1) = 0$. Also, we notice that conservation of center of mass implies, by integrating Eq. (7) over contour position: $\zeta_c^2[\mathbf{x}'(1) - \mathbf{x}'(0)] = \int_0^1 \mathbf{x}(s) - \mathbf{x}^o(s)\,\mathrm{d}s \propto \mathbf{x}_{cm} - \mathbf{x}_{cm}^o = 0$. The latter condition serves to obtain slightly modified boundary conditions, but both versions only differ in a correction of order $1/N$, which is irrelevant for long chains. The projection has the following invariant features $\mathbf{x}(0) + \mathbf{x}(1) = \mathbf{x}^o(0) + \mathbf{x}^o(1)$, $\mathbf{l}(1) = \mathbf{l}(0)$, $\langle\mathbf{x}\rangle = \langle\mathbf{x}^o\rangle$, and $\langle\mathbf{Q}\cdot\mathbf{l}\rangle = 0$, where the latter relationship representing a vanishing torque follows by multiplication of Eq. (7) with $\mathbf{l}$ and subsequent integration. In the above $\langle f\rangle$ abbreviates the average $\langle f\rangle = \int f(s)\,\mathrm{d}s \approx 1/N\sum_i f_i$. According to the boundary conditions conservation of the

end-to-end vector $\mathbf{R} = \mathbf{R}^0$ requires $\zeta_c = 0$, and for an atomistic rod, e.g. we have $\mathbf{R}^0 - \mathbf{R} = 2N\zeta_c^2 \mathbf{1}(0)$.

3.1. Analytic solution

Coordinates of the PP. In order to solve Eq. (7) subjected to the above boundary conditions we make use of the appropriate Green's function and thus obtain the continuous form of the projection operator $\mathscr{P}$ with $\mathbf{x}(s) = \int \mathscr{P}_\zeta(s,s')\mathbf{x}^o(s')\,ds'$. With this projection operator at hand, we also have access to an approximate explicit form of the projection matrix. The solution for the PP reads

$$\mathbf{x}(s) = \frac{G_1(s)}{G_2(1)} F[\mathbf{x}^o] + \int_0^s \mathbf{x}^o(t) G_0(t-s)\,dt + \mathbf{x}^o(0), \tag{8}$$

where $F[\mathbf{x}^o] \equiv \mathbf{x}^o(1) + \int_0^1 \mathbf{x}^o(t) G_1(1-t)\,dt$. The following abbreviation turned out to be useful:

$$G_\nu(z) \equiv \frac{1}{2\zeta_c}[(1+\zeta)^\nu\, e^{z/\zeta_c} - (1-\zeta)^\nu\, e^{-z/\zeta_c}], \tag{9}$$

again, with $\zeta = N\zeta_c$ as before. Note that $G_1(0) = N$ and $G_0(z) = -G_0(-z) = \sinh(z/\zeta_c)\zeta_c^{-1}$. For the semiflexible case with $\zeta \gg 1$ one has: $G_2(z) = \zeta^2 G_0(z)$ and $G_1(z) = N\cosh(z/\zeta_c)$ whereas in the stiff limit $\zeta_c \gg 1$ the expressions further simplify due to: $G_0(z) = z\zeta_c^{-2}$, $G_1(z) = N$, and $G_2(z) = N^2 z$.

As will be shown below, in practice, considering the analytic result for the semiflexible limit $\zeta \gg 1$ will be sufficient in many cases. For that reason we write the result down explicitly, this time for the projector:

$$\mathscr{P}_\zeta(s,s') = \frac{\cosh(s/\zeta_c)}{\zeta \sinh(\zeta_c^{-1})}\left[\delta(1-s') + N\cosh\left(\frac{1-s'}{\zeta_c}\right)\right] - \Theta(s-s')\frac{1}{\zeta_c}\sinh\left(\frac{s-s'}{\zeta_c}\right). \tag{10}$$

This expression shows that the projection can be rewritten into products which either depend on s or s', and that the projection matrix can be also decomposed into a sum of matrix multiplications (which would not serve to enhance the speed of an algorithm).

End-to-end vector. For the end-to-end vector of the PP $\mathbf{R} \equiv \mathbf{x}(1) - \mathbf{x}(0) \equiv \int_0^1 \mathbf{l}(s)\,ds$ we obtain from Eq. (8)

$$\mathbf{R} = \int_0^1 (G_0(t) + \alpha[G_1(t) + \delta(t)])\mathbf{x}^o(1-t)\,dt, \tag{11}$$

with $\alpha \equiv [G_1(1) - G_1(0)]/G_2(1)$. For the case of the rods, $\alpha = 0$, and the PP shrinks into a single point for $\zeta \to \infty$ (the center of mass of the atomistic chain), due to $\mathbf{R} = \zeta_c^{-2}\int_0^1 (t-1)\mathbf{x}^o(t)\,dt \propto \zeta_c^{-2}$ for large ζ_c.

Tangent vectors of the PP. The tangent vectors $\mathbf{l}(s)$ of the PP at contour position s satisfy the differential equation $\zeta_c^2\mathbf{l}'' - \mathbf{l} = -\mathbf{l}^o$, with two boundary conditions $(1+\zeta^2)\mathbf{l}(0) = \mathbf{l}^o(1) - N\zeta_c^2\mathbf{l}'(1)$ and $(1+\zeta^2)\mathbf{l}(1) = \mathbf{l}^o(1) - N\zeta_c^2\mathbf{l}'(1)$. These equations are obtained from the discrete version cf. Eq. (2), rewritten as $(1+2\zeta^2)\mathbf{l}_i = \mathbf{l}_i^o + \zeta^2(\mathbf{l}_{i+1} + \mathbf{l}_{i-1})$. Using once more the appropriate Green's function, the solution of the differential equation for $\mathbf{l}'$, subjected to the above boundary conditions reads

$$\mathbf{l}(s) = \int_0^s \frac{\sinh(t - s/\zeta_c)}{\zeta_c}\mathbf{l}^0(t)\,dt + \alpha_-(s-1)\mathbf{l}^0(0)\alpha_+(s)\mathbf{l}^0(1) + \frac{\alpha_+}{\zeta_c}\int_0^1 \mathbf{l}^0(t)\Gamma_-(t-1)\,dt, \tag{12}$$

or alternatively

$$\mathbf{l}(s) = \int_0^1 \mathscr{L}_\zeta(s,s')\mathbf{l}^0(s')\,ds', \tag{13}$$

with the following kernel

$$\mathscr{L}_\zeta(s,s') = \Theta(s-s')\frac{1}{\zeta_c}\sinh\left(\frac{s-s'}{\zeta_c}\right) + \alpha_-(s-1)\delta_{s',0} - \alpha_+(s)\delta_{s',1} + \alpha_+(s)\frac{\Gamma_-(s'-1)}{\zeta_c}. \tag{14}$$

Here, $\Theta(x)$ denotes the Heaviside step function $\Theta(x) = 1$ for $x \le 0$ and $\Theta(x) = 0$ otherwise, and the abbreviations

$$\Gamma_\pm(t) \equiv (1+\zeta^2)\sinh(t/\zeta_c) \pm \zeta\cosh(t/\zeta_c),$$

$$\alpha_\pm \equiv \frac{2}{W}\Gamma_\pm(t), \tag{15}$$

$$W \equiv (1+\zeta^2-\zeta)^2\, e^{-1/\zeta_c} - (1+\zeta^2+\zeta)^2\, e^{1/\zeta_c}$$

have been used. With Eq. (14) at hand, we can most easily derive expressions for the average bond length, the persistence length, and correlations in general.

Correlations. One usually does not have access to the atomistic conformation $\mathbf{x}^o(s)$, but information about correlations of tangent vectors. From Eqs. (13) and (14) we obtain for the tangent–tangent correlation matrix

$$\mathbf{C}(\Delta s) \equiv \int \mathbf{l}(s)\mathbf{l}(s+\Delta s)\,ds = \left\langle \mathscr{L}_\zeta(s,s')\int_{-s'}^{1-s'} \mathscr{L}_\zeta(s+\Delta s, s'+z)\mathbf{C}^0(z)\,dz \right\rangle, \tag{16}$$

where $\langle\rangle$ denotes a twofold integration over s and s', and the tangent–tangent correlation on the atomistic scale is expressed by $\mathbf{C}^0(z) = \int \mathbf{l}^0(s)\mathbf{l}^0(s+z)\,ds$, whenever end effects can be neglected, as for the FJC, which is completely characterized through (dimension d)

$$\mathbf{C}^0(\Delta s) = \langle R^{o^2}\rangle \delta(\Delta s)\mathbf{I}/d. \tag{17}$$

Contour length of the PP. For example, the average squared bond length b_2 vs. contour position for FJC is

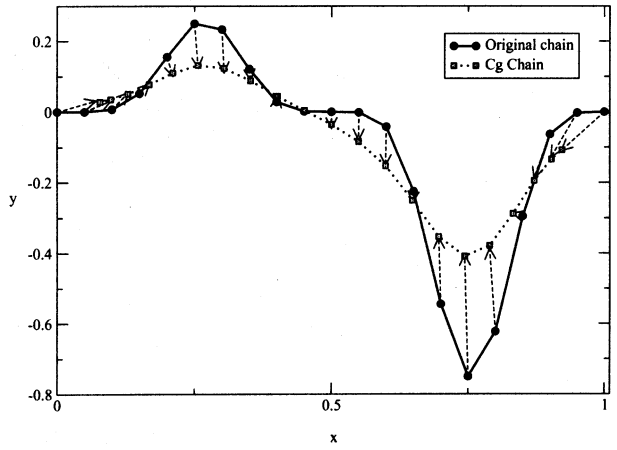

Fig. 3. Displacement of selected points on the two-dimensional sample contour (21) due to the continuous mapping procedure for chosen mapping parameter $\zeta_c = 0.1$ (and $N \to \infty$).

obtained via

$$b_2 \equiv \langle \mathbf{l}(s)\cdot\mathbf{l}(s)\rangle = \int\int \mathscr{L}^2_\zeta(s,t)\,\mathrm{d}t\,\mathrm{d}s\langle R^{o^2}\rangle, \tag{18}$$

with the following kernel

$$\begin{aligned} \mathrm{L}^2_\zeta(s,t) = \frac{2}{\zeta_c}\Bigg[& \frac{1}{2\zeta_c}\sinh^2\left(\frac{t-s}{\zeta_c}\right) - \sinh\left(\frac{s}{\zeta_c}\right)\alpha_-(s-1) \\ & + \frac{1}{\zeta_c}\sinh\left(\frac{t-s}{\zeta_c}\right)\Gamma_-(t-1)\alpha_+(s) \\ & + \alpha_-(s-1)\alpha_+(s)\Gamma_-(-1) - \alpha^2_+(s)\Gamma_-(0)\Bigg] \\ & \times \Theta(t-s) + \frac{\alpha^2_+(s)}{\zeta^2_c}\Gamma^2_-(t-1). \end{aligned} \tag{19}$$

In the semiflexible case $\zeta \gg 1$ the integral can be explicitly evaluated to yield

$$\frac{b_2}{\langle R^{o^2}\rangle} = \frac{[\cosh(2/\zeta_c) + \sinh(2/\zeta_c)][\zeta_c \sinh(2/\zeta_c) - 2]^2}{[2(\mathrm{e}^{2/\zeta_c} - 1)\zeta_c]^2}, \tag{20}$$

which is a decreasing function in ζ_c, otherwise sine integrals remain. Similarly, the contour length or persistence lengths can be evaluated. The latter quantity, e.g. by comparing the squared end-to-end distance with the expression by Flory or Kratky [16,17].

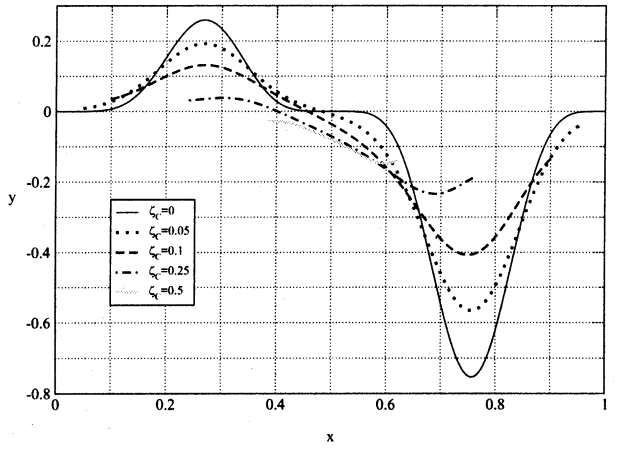

Fig. 4. Coarse-graining as for Fig. 3 for different mapping parameters ζ_c.

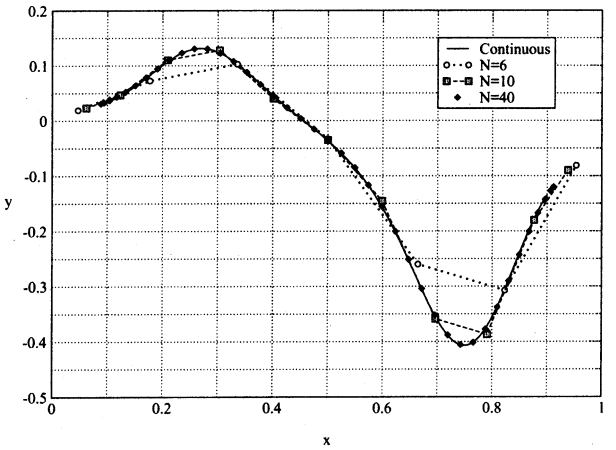

Fig. 5. Comparison between discrete (several N) and continuous mapping ($N \to \infty$) for $\zeta_c = 0.1$, again for the atomistic chain defined by Eq. (21).

4. An illustrative example

In this section we apply both procedures, the continuous and the discrete one to a particular conformation in order to illustrate that the continuous solution indeed represents the limit of the discrete one for an infinite number of beads. For this purpose let us regard the following two-dimensional path, parameterized by s

$$x(s) = s, \qquad y(s) = s\sin^5(2\pi s). \tag{21}$$

Fig. 3 demonstrates how the atomistic ('original') continuous chain, expressed by Eq. (21), displaces according to the continuous mapping to yield the continuous PP (here for $\zeta_c = 0.1$). The effect of the mapping parameter ζ_c on the shape of the PP for the fixed atomistic contour (recovered for $\zeta_c = 0$) is depicted in Fig. 4. It is visible that the parameter ζ_c controls the stiffness of the coarse grained PP.

Now we use the same continuous atomistic curve to build a series of discrete chains, by selecting a prescribed number $N + 1$ of points along the path and taking them equidistant in terms of the contour position s. In Fig. 5 we compare the discrete coarse graining to the continuous one with the same value for ζ_c (and therefore different values for ζ), to visualize the effect of the chosen number of beads. For this simple curve, we see that the discrete mapping tends to the continuous one as the number of beads increases, as expected.

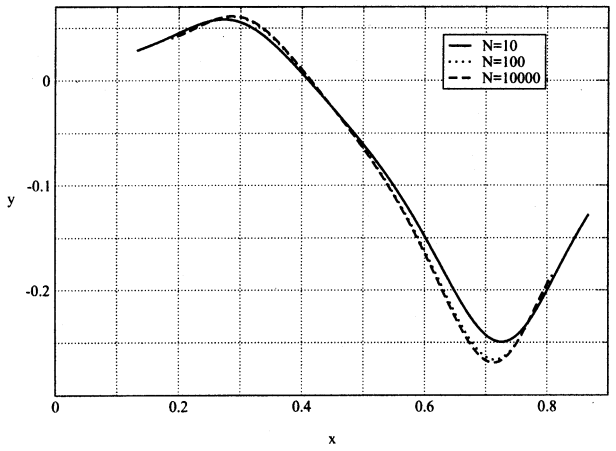

Fig. 6. Effect of N on the boundary condition, and thus the solution for the continuous PP, for $\zeta_c = 0.2$.

Since N appears in the boundary condition for the continuous curve, we wish to clarify how the continuous solution is affected by a different choice of N. Fig. 6 therefore demonstrates how the continuous solution converges with increasing value N for fixed ζ_c.

5. Properties of the discrete PP

Starting from Eqs. (4) and (5) for the discrete PP, we can evaluate and analyze expressions for a number of descriptors. The end-to-end vector is defined as $\mathbf{R} = \sum_{i=1}^{N} \mathbf{l}_i$, and the end-to-end distance then reads

$$R^2 = \sum_{i,j} \mathbf{l}_i \cdot \mathbf{l}_j \equiv \sum_{i,j} (\mathbf{l}\mathbf{l}^{\mathrm{T}})_{ij}. \tag{22}$$

From Eq. (4) we obtain

$$\mathbf{l}\mathbf{l}^{\mathrm{T}} = \mathbf{A}^{-1} \cdot (\mathbf{l}^{\mathrm{o}}\mathbf{l}^{\mathrm{o}^{\mathrm{T}}}) \cdot \mathbf{A}^{-1}, \tag{23}$$

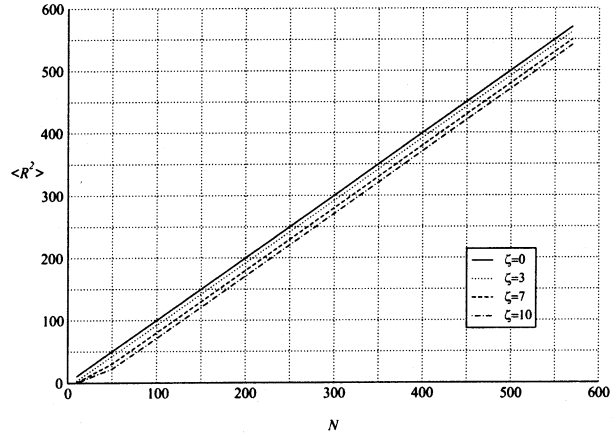

Fig. 7. Effect of ζ on the squared end-to-end distance $\langle R^2 \rangle$ of the FJC-PP. Here and in the following figures quantities (such as R^2, l_p, Q) are made dimensionless for convenience, by the (unit) bond length b_0 of the atomistic chain.

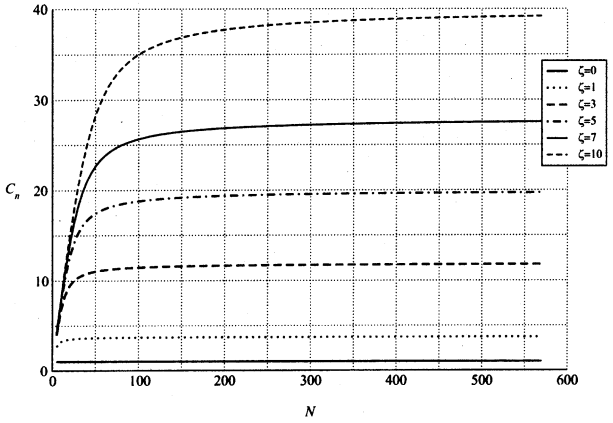

Fig. 8. Effect of ζ on the characteristic ratio of the FJC-PP.

where the dyadic product of the vectors $\mathbf{l}^{\mathrm{o}}$ and $\mathbf{l}^{\mathrm{o}^{\mathrm{T}}}$ is a tensor of second order whose elements are the scalar products $\mathbf{l}_i^{\mathrm{o}} \cdot \mathbf{l}_j^{\mathrm{o}}$. We have also made use of the symmetry of the matrix $\mathbf{A}$, and therefore of $\mathbf{A}^{-1}$. From $\langle R^2 \rangle$, together with

$$N\langle l^2 \rangle = \sum_{i,j} (\mathbf{A}^{-2})_{ij} \langle \mathbf{l}_i^{\mathrm{o}} \cdot \mathbf{l}_j^{\mathrm{o}} \rangle, \tag{24}$$

We can evaluate the characteristic ratio $C_n = \langle R^2 \rangle / N\langle l^2 \rangle$.

For FJC, characterized by $\langle \mathbf{l}^{\mathrm{o}}\mathbf{l}^{\mathrm{o}^{\mathrm{T}}} \rangle = l^2\mathbf{1}$, the resulting end-to-end distance is $\langle R^2 \rangle = l^2 \sum_{i,j} (\mathbf{A}^{-2})_{ij}$, and the characteristic ratio C_n of the FJC-PP (PP obtained for the FJC) expresses as

$$C_n = \frac{\sum_{i,j} (\mathbf{A}^{-2})_{ij}}{\mathrm{Tr}[\mathbf{A}^{-2}]}. \tag{25}$$

It is not possible to evaluate $\mathbf{A}^{-1}$ or $\mathbf{A}^{-2}$ analytically for all ζ, ζ_c, but we evaluate these expressions numerically. From Fig. 7 it is then visible that the value for ζ (at given N) does not affect much the FJC-PP squared end to end distance, the value still scales with N. Fig. 8 shows the effect of ζ on C_n for different chain lengths N. The behavior of this plot can be generalized for almost all the geometrical descriptors to be discussed in this section. Each descriptor rises up until it reaches a well defined plateau for very long chains, and thus we can create plots for the extracted limiting values of the different quantities against ζ. In Figs. 9 and 10 we see that C_n scales almost linearly with the parameter ζ, using Eq. (25) for FJC, using the corresponding expression for the freely rotating chain, and using a set of configurations of linear long chains well relaxed by end-bridging Monte Carlo simulation [18]. From Figs. 7 and 10 we can extract the following information. The squared end-to-end distance is proportional to N and essentially insensitive to the value for ζ. The characteristic ratio C_n increases linearly with ζ. This behavior is expected for the proper projection, with increasing ζ it makes the PP stiffer but approximately maintains the end-to-end distance, while kinks are steadily removed from the PP.

The squared radius of gyration s^2 of a chain molecule [16]

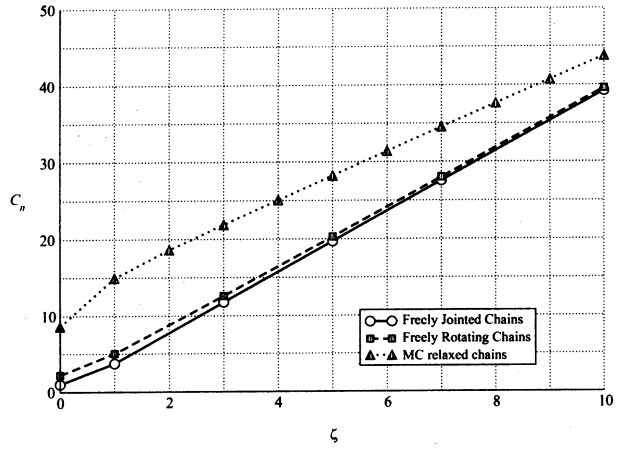

Fig. 9. Characteristic ratio C_n for FJC-PP as function of ζ.

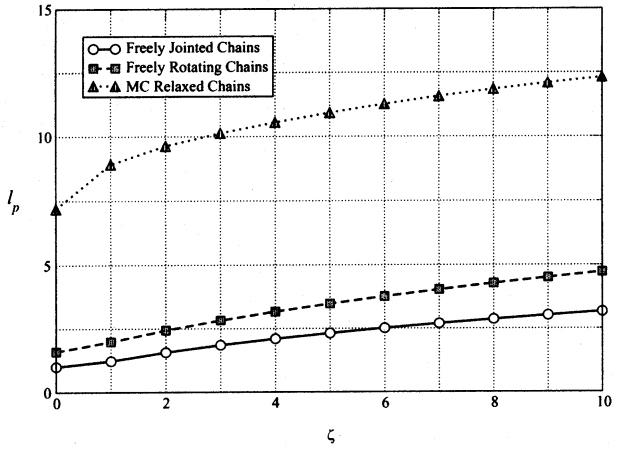

Fig. 11. Persistence length l_p (Eq. (28)) vs. ζ for the FJC-PP.

is defined as $s^2 = \sum_{i<j} [\mathbf{x}_i - \mathbf{x}_j]^2/N^2$. Proceeding as in the previous case, we finally get

$$\langle s^2 \rangle = \frac{1}{N^2} \sum_{i \le j} \sum_{k,m=i}^{j} \langle \mathbf{l}\mathbf{l}^{\mathrm{T}}_{km} \rangle, \tag{26}$$

that, in the case of the FJC model, reduces to

$$\langle s^2 \rangle = \frac{l^2}{N^2} \sum_{i \le j} \sum_{k,m=i}^{j} (\mathbf{A}^{-2})_{km}. \tag{27}$$

We can further apply the definition given by Porod [19] for the persistence length l_p though it is intended for being used only with bonds far from both ends of the chain. The definition reads

$$l_p = \frac{1}{N} \sum_{i=1}^{N} \frac{1}{l_i} \sum_{j=1}^{N} (\mathbf{l}_i \cdot \mathbf{l}_j). \tag{28}$$

In order to average this expression, we make the following approximation $\langle l_i \rangle \approx \sqrt{\langle l^2 \rangle}$, and finally obtain

$$\langle l_p \rangle = \frac{1}{N} \frac{1}{\langle l_i \rangle} \sum_{i \le j} \langle \mathbf{l}\mathbf{l}^{\mathrm{T}}_{ij} \rangle, \tag{29}$$

which, for the FJC case simplifies to

$$\langle l_p \rangle = \frac{l}{\sqrt{N \,\mathrm{Tr}[\mathbf{A}^{-2}]}} \sum_{i \le j} (\mathbf{A}^{-2})_{ij}. \tag{30}$$

Figs. 11 and 12 demonstrate that the relation between l_p and ζ is sublinear, for $\zeta \to 0$ we recover the persistence length of the atomistic chain. We do not show the corresponding plot here but we convinced ourself that $C_n = 2l_p/\langle l \rangle - 1$ holds, with $\langle l \rangle = 1/N \sum_1^N l_i$. Notice, that due to the coarse graining the bond length distribution is not uniform along the PP, such that the average bond length and the average squared bond length (involved in the calculation of the characteristic ratio) of the PP depend differently on the parameter of the projection. Thus $C_n$and l_p scale differently with ζ. We may further apply the definition of a 'step length' a given by Doi and Edwards [14], $\langle (\mathbf{R}(s,t) - \mathbf{R}(s',t))^2 \rangle = a|s - s'|$, for $|s - s'| \gg a$. We can approximate

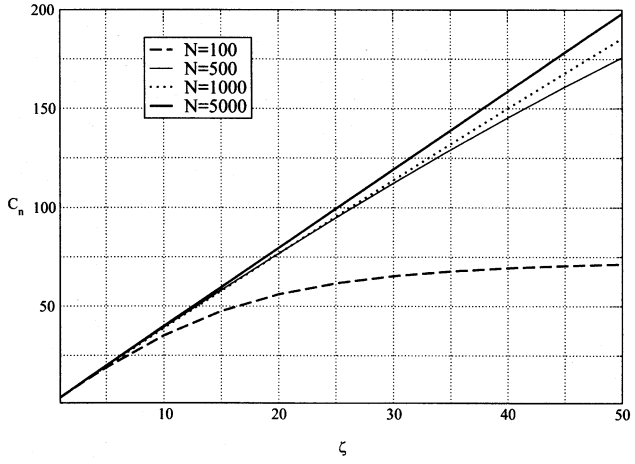

Fig. 10. Characteristic ratio C_n for FJC-PP as function of ζ as for the previous figure, but for a larger ζ-range.

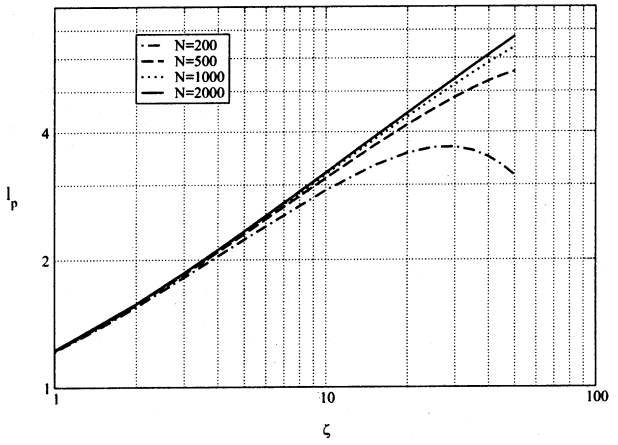

Fig. 12. Persistence length l_p extracted according to expression (28) vs. ζ in double logarithmic representation for the FJC-PP.

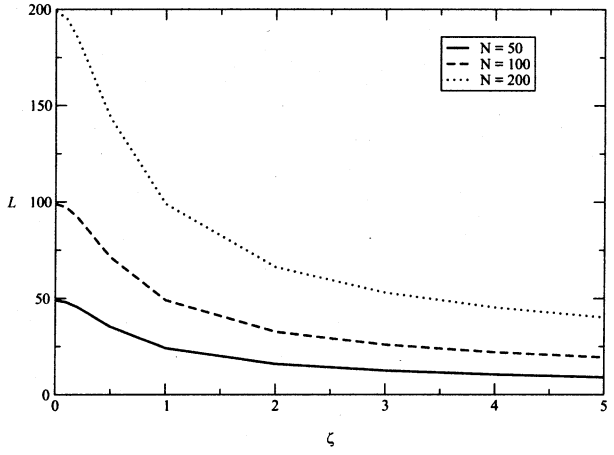

Fig. 13. Average contour length $L = \langle \sum |\mathbf{l}_i| \rangle$ of FJC-PP chains vs. ζ for $N =$ 50, 100, 200 beads (10^5 chains samples). Obviously, the average bond length L/N is quite insensitive to N (compare also with subsequent figures).

the step length of the coarse grained chain by $a = \langle R^2 \rangle / \langle L \rangle$, where $\langle L \rangle = N \langle l_i \rangle$ (see also Fig. 13). The explicit expression for the step length in terms of $\mathbf{A}$ and the tangent–tangent correlation of the atomistic chain reads

$$a = \frac{\sum_{i,j} \langle \mathbf{l}\mathbf{l}_{ij}^{\mathrm{T}} \rangle}{\sqrt{N \sum_{i,j} (\mathbf{A}^{-2})_{ij} \langle \mathbf{l}_i^{\mathrm{o}} \cdot \mathbf{l}_j^{\mathrm{o}} \rangle}}, \tag{31}$$

that, in the particular case of a FJC, reduces to

$$a = \frac{l \sum_{i,j} (\mathbf{A}^{-2})_{ij}}{\sqrt{N \, \mathrm{Tr}[\mathbf{A}^{-2}]}}. \tag{32}$$

Finally, we calculate the mean squared 'tube radius' based on the tube vectors $\mathbf{Q}_i$ defined in Eq. (5). In terms of $\mathbf{A}$ and the atomistic tangent–tangent correlation,

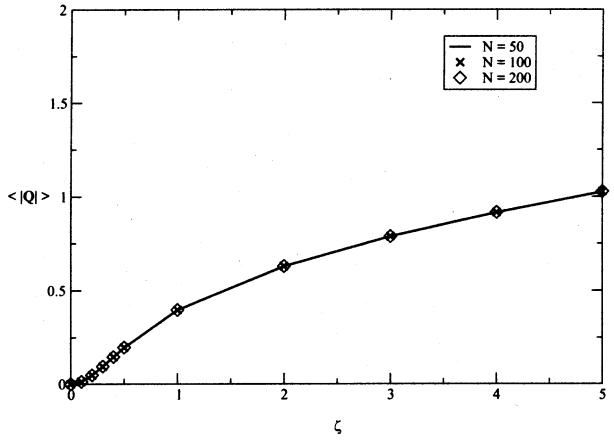

Fig. 14. Effect of ζ on the average tube radius $\langle |\mathbf{Q}| \rangle$ of FJC-PP.

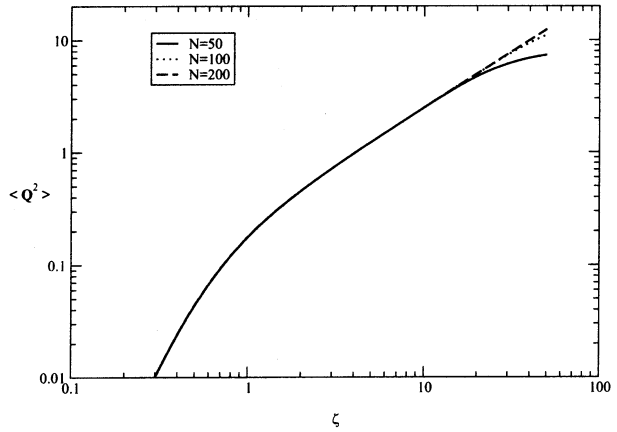

Fig. 15. Average squared tube radius $\langle \mathbf{Q}^2 \rangle$ vs. ζ for the FJC-PP in double logarithmic representation.

it reads

$$\langle Q^2 \rangle = \sum_{i,j} \frac{(\mathbf{A}^{-1} \cdot \mathbf{D}^{\mathrm{T}} \cdot \mathbf{D} \cdot \mathbf{A}^{-1})_{ij}}{N+1} \langle \mathbf{l}_i^{\mathrm{o}} \cdot \mathbf{l}_j^{\mathrm{o}} \rangle, \tag{33}$$

and, once more, for the particular case of the FJC-PP

$$\langle Q^2 \rangle = \frac{l^2}{N+1} \mathrm{Tr}[\mathbf{A}^{-1} \cdot \mathbf{D}^{\mathrm{T}} \cdot \mathbf{D} \cdot \mathbf{A}^{-1}]. \tag{34}$$

For a quantitative analysis see Figs. 14–17. The tube radius, for flexible and semiflexible PPs is insensitive to the value for N, and reaches a limit which of course depends on the chain length in the stiff limit, because for $\zeta \to \infty$, the tube radius becomes equivalent to the radius of gyration of the atomistic chain.

Finally, our approach also allows to extract a tube volume V and to relate it to the parameter of the projection ζ, or quantities related to ζ, such as tube diameter or the persistence length. In first approximation the tube volume may be expressed as the product between tube cross-section Eq. (34)

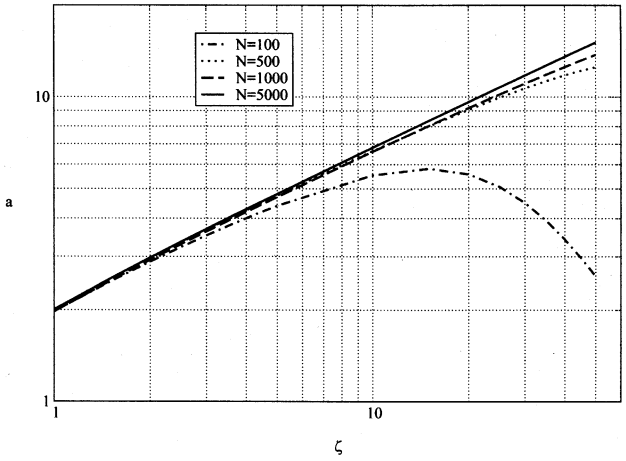

Fig. 16. Step length a of the PP vs. parameter of the projection ζ for the FJC-PP. In the long chain limit we have $a \propto \sqrt{\zeta b_0}$.

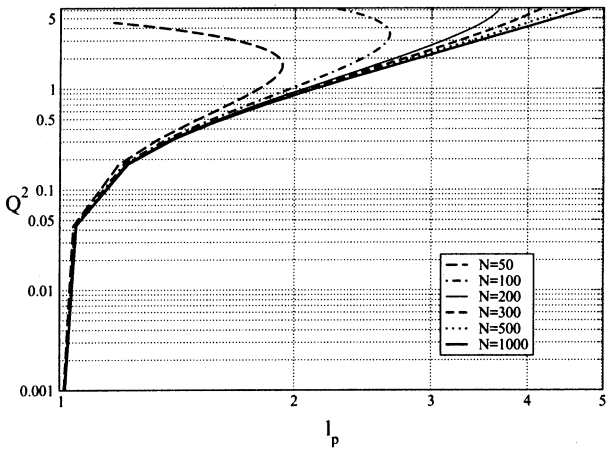

Fig. 17. Squared 'tube radius' Q^2 vs. the persistence length l_p.

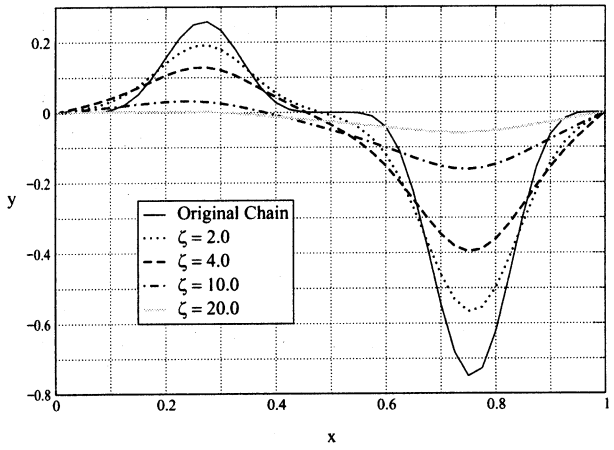

Fig. 19. Same situation as in Fig. 4 but with the ends fixed. The length of the chain is $N = 40$.

and length of the PP, i.e. $V \propto LQ^2$. From the investigations above we know that we have for long chains $Q^2 \propto \zeta b_0^2$ (see Fig. 18), and that the step length increases with ζ, viz. $a \propto \zeta^x b_0$, with $x \approx 1/2$. Together with the relationship $La = Nb_0^2$ we obtain an expression for the tube volume: $V \propto Nb_0^3\zeta^{1-x}$. Since $x \neq 1$, also the tube volume should depend on the parameter of the projection, and because the persistence length has been shown to scale with ζ as a does, the volume of our PP can be also expressed as: $V \propto Nb_0^2 l_p$. The shrinking of the PP upon increasing ζ therefore compensates for the increase of tube cross section, such that the growth of tube volume is in fact moderate.

6. Variations of the model

As can be seen in Fig. 4, the proposed projection is only weakly influenced by the exact position of the ends of the atomistic chain. The PP tends to shrink as the parameter ζ increases and its ends eventually separate more and more from the corresponding ends of the atomistic chain. Although the very end beads of an atomistic chain should not be thought to build up an entanglement segment, our projection may be considered as an 'inconvenient' representation of a PP, beyond the above discussion of tube volume. To prevent the chain from shrinking upon increasing the parameter ζ, two alternative approaches will be shortly discussed.

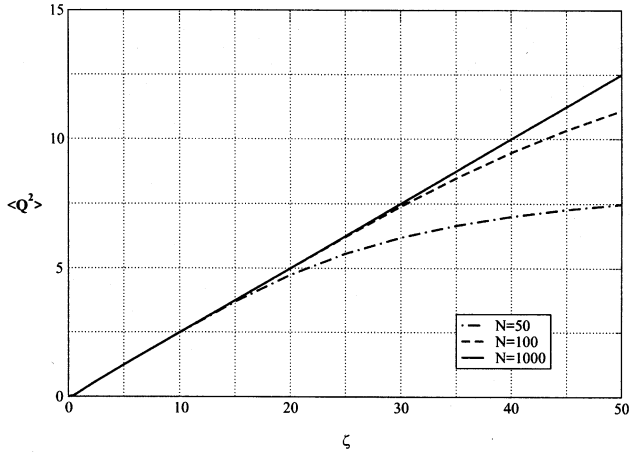

Fig. 18. Squared tube radius Q^2 vs. ζ for the FJC-PP. For infinitely long chains a linear relationship between squared tube diameter $2Q$ and ζ is obtained, viz. $\langle(2Q)^2\rangle = \zeta b_0^2$ where b_0 is the atomistic bond length. Therefore the parameter ζ, a ratio between spring coefficients in the microscopic picture, shows up as a dimensionless tube cross section.

6.1. Chain ends fixed

The first and simplest way to prevent the ends of the PP from separating too much from the ends of the atomistic chain is — of course — to fix them. If the projected beads at the ends of the PP are kept tethered at the end beads of the original atomistic chain, the projection matrix has also a tridiagonal structure, very similar to Eq. (3). It can still be inverted in $O(N^1)$ operations and the efficience of the method is not diminished.

In Fig. 19 it is shown how the mapping is affected by this modification: the structure of the PP is determined by the fluctuating location of the atomistic chain ends. This is in fact against the spirit of the coarse graining. A structure defined in an upper level of description should not be so much determined by information from a lower level, and we do not need to consider this approach further.

6.2. Maxwell Daemon

The second possibility to circumvent shrinking is to introduce a Maxwell daemon acting at both ends of the projected chain. The daemon induces tension along the PP and tends to keep its ends closer to those of the original chain. It has been implemented as a force of constant strength (depending of the temperature, reflecting entropic spring effects) having the direction of the last bond of the PP, pulling out the ends. The expressions for the forces at both ends are

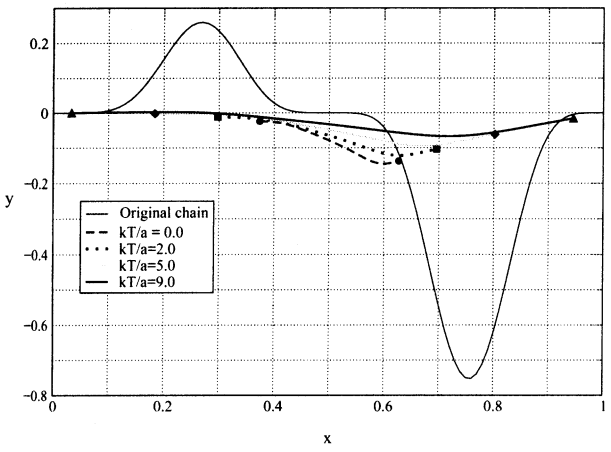

Fig. 20. Same situation as in Fig. 4, for the case $\zeta_c = 0.5$, using a Maxwellian Daemon. The length of the chain is $N = 40$. The ends of the chains are represented by symbols.

then

$$\mathscr{F}_0 = \frac{k_B T}{a} \frac{\mathbf{x}_0 - \mathbf{x}_1}{|\mathbf{x}_0 - \mathbf{x}_1|}, \qquad \mathscr{F}_N = \frac{k_B T}{a} \frac{\mathbf{x}_N - \mathbf{x}_{N-1}}{|\mathbf{x}_N - \mathbf{x}_{N-1}|}, \quad (35)$$

at ends 0 and N, respectively. The daemon cannot be derived from a potential and it leads to a non-linear system of equations to be solved (numerically) in order to perform the new projection.

The equations for beads 0 and N now read

$$\begin{aligned} (\mathbf{x}_0 - \mathbf{x}_0^o) - \zeta^2 \mathbf{l}_1 - \mathscr{F}_0 = 0, \\ (\mathbf{x}_N - \mathbf{x}_N^o) - \zeta^2 \mathbf{l}_N - \mathscr{F}_N = 0. \end{aligned} \quad (36)$$

The expressions for all remaining beads do not change, cf. Eq. (2). To solve this system of equations, the Newton–Raphson method has been used, and the modification has been tested on the example of Fig. 4, for the case of $\zeta_c = 0.5$. In Fig. 20 it is shown, for different values of the parameter $k_B T/a$, how this modification can vary the result of the mapping. This parameter may be also selfconsistently determined such that the end-to-end distance of the PP equals the one of the atomistic chain. Using the Maxwell daemon, chain end effects are less pronounced than for the 'fixed ends' method. A drawback is that the speed of the algorithm is decreased. The average number of iterations that need to be done in the Newton–Raphson method for solving the non-linear system of equations is independent of the parameter ζ, but it increases linearly with the value of the parameter $k_B T/a$. The method requires, beside ζ, the step length a, which in turn depends on ζ. This appears to be inconvenient in defining a PP, but may serve to interpret an effect of temperature on the properties of the PP.

7. Conclusions and outlook

In this note we presented and motivated a possible definition for the PP of an 'atomistic' (discrete or continuous) linear polymer chain, based on the space coordinates of that atomistic chain, and parameterized by a single parameter (ζ).

The original idea of Doi and Edwards introduces the PP using two interrelated quantitites, the length L and the step length a of the PP. One of them is a priori unknown. In our approach the ratio of spring coefficients ζ is the only parameter of the microscopically founded PP, from which the length L of the PP, and the step length $a = Nb_0^2/L$ are obtained as function of ζ (and chain length N). Moreover, our approach allows to interpret the step length a, e.g. in terms of the persistence length of the PP. Due to the microscopic definition of the PP only the long chain limit provides universal results to be compared with the setup of the original PP concept. It therefore allows to interpret 'anomalies' for short chains, or the effect of temperature through a Maxwell daemon, as outlined above.

For the case of atomistic freely jointed chain (FJC) we demonstrated, that our parameter ζ scales linearly with the characteristic ratio of the PP, and we investigated the effect of ζ on several conformational properties such as the contour length, or tube diameter of the PP. It turned out that all investigated quantities depend monotonically (and nonlinearly) on ζ, and thus serve to characterize the projection as well. For example, stiffening of the PP comes together with a shrinking of the contour length, but — in view of the original tube picture of Doi and Edwards, one may wish to fix the contour length as an independent parameter of the projection. This can be achieved, e.g. by further introducing a Maxwell Daemon (with fixed strength according to a given temperature) pulling at the ends of the PP in direction of the final segments, while preserving the contour length by adjusting ζ. By means of our treatment of the continuous PP it was shown that these segments are parallel to each other, such that a Maxwell daemon would not tend to rotate the chain, but stretch out the segments close to the ends of the PP. Of course, since the system of equations for the contour of the PP becomes non-linear in that case, the computational effort strongly increases (in fact it increases linearly with temperature).

The proposed (linear) projection to a PP is easily implemented such that it scales linearly with the number of beads, and therefore allows for its evaluation during a Monte Carlo simulation. As shortly discussed above, there is ongoing research in the direction of using information about the conformation of PP (and other coarse-grained quantities) for generalized canonical Monte Carlo simulations [10].

There is another aspect to be shortly mentioned. In the theory of anisotropic tube cross-sections [20,21] it had been proposed that during deformation an initial circular tube cross section may become elliptical, while the so called stress-optic rule is preserved [20]. In Ref. [22] a dynamic equation for a certain quantity $\mathbf{Q}$ had been proposed which enabled to interpret the stress tensor proposed in Ref. [20],

but the physical meaning of $\mathbf{Q}$ still remains open. All we expect about $\mathbf{Q}$ is its equation of change

$$\dot{\mathbf{Q}} = -(1 - \alpha\mathbf{qq})\cdot\kappa^{\dagger}\cdot\mathbf{Q} - \beta(\kappa : \mathbf{uu})\mathbf{Q}, \tag{37}$$

with the following solution: $\mathbf{Q}(t) \propto \tilde{\mathbf{E}}\cdot\mathbf{Q}_0$ where $\mathbf{Q}_0 = \mathbf{Q}(0)$ and a proportionality coefficient due to

$$|\mathbf{Q}|(t) = Q_0^{\alpha}|\tilde{\mathbf{E}}\cdot\mathbf{Q}_0|^{1-\alpha}|\mathbf{E}\cdot\mathbf{u}_0|^{-\beta}, \tag{38}$$

since $\dot{Q} = -Q\kappa : [\beta\mathbf{uu} + (1 - \alpha)\mathbf{qq}]$. Here, α and β are yet unknown coefficients of the anisotropic tube model, $\kappa \equiv (\nabla\mathbf{v})^{\dagger}$ denotes deformation rate tensor, $Q \equiv |\mathbf{Q}|$, $\mathbf{q} \equiv \mathbf{Q}/Q$, and $\tilde{\mathbf{E}} = \tilde{\mathbf{E}}(t) = \exp(-\kappa^{\dagger}t)$. From the proportionality between $\mathbf{Q}$ and $\tilde{\mathbf{E}}\cdot\mathbf{Q}_0$ follows directly, that the inner product $\mathbf{u}\cdot\mathbf{Q}$ is conserved, as long as $\mathbf{u}$ denotes a segment which is pseudo-affinely deformed, i.e. $\mathbf{u}(t) = \mathbf{E}\cdot\mathbf{u}_0/|\mathbf{E}\cdot\mathbf{u}_0|$ with the finite strain tensor $\mathbf{E} = \exp(t\kappa) = (1 + t\kappa + \cdots)$. For shear flow, we simply have: $\mathbf{E}|_{\text{shear}} = (1 + t\kappa)$. Our hope is to extract the coefficients α, β by using the definition of a PP, because the model equations for anisotropic tubes were considered to be applicable for quantities which represent atomistic chains on a coarse-grained level with specified contour length. In order to estimate the coefficients α, β of the model, we need to investigate the convective motion of an underlying atomistic chain, which allows to extract $\mathbf{u}$ (tangential to the PP) and $\mathbf{Q}$ (for example, as defined in Eq. (5)) for given (small) deformation κt. The described procedure allows to extract arbitrary ensemble averages which involve contour and tube vectors. These averages have to be compared with the ones predicted in connection with Eq. (37). In order to illustrate the procedure, let us write down a sample relationship between ensemble averages, derived from the corresponding convective part of the diffusion equation

$$\frac{\mathrm{d}}{\mathrm{d}t}\langle Q_\mu Q'_\nu\rangle = -[\kappa_{\mu\lambda}\langle Q_\lambda Q_\nu\rangle + \langle Q_\mu Q_\lambda\rangle\kappa^{\mathrm{T}}_{\lambda\nu} - 2\langle Q_\mu Q_\nu(\alpha\mathbf{qq} - \beta\mathbf{uu})\rangle : \kappa]. \tag{39}$$

It is visible that the tube cross section is always circular for $\alpha = 1$, $\beta = 0$, and it will be interesting to analyze these parameters as a function of our model parameter ζ in order to see if the ratio between second and first normal stress difference, extensively discussed [5–7,14,17,20,21,23] — and predicted to behave as $\Psi_2/\Psi_1 = -2/7[(1 + \beta + 5/2\alpha)/(1 + \alpha + \beta)]$ — depends on ζ, and if experimentally measured values $\Psi_2/\Psi_1 \approx -1/4$ can be interpreted by the help of the hereby introduced PP.

References

[1] Lee S, Mattice WL. Comput Theor Polym Sci 1999;9:57.
[2] Kröger M, Voigt H. Macromol Theory Simul 1994;3:639.
[3] Kröger M, Hess S. Phys Rev Lett 2000;85:1128.
[4] Khodolenko AL, Vilgis TA. Phys Rep 1998;298:251.
[5] Doi M, Edwards SF. J Chem Soc Faraday Trans 1978;74:1789, also p. 1802, 1818.
[6] Doi M, Edwards SF. J Chem Soc Faraday Trans 1979;75:38.
[7] Marrucci G, Greco F, Ianniruberto G. Curr Opin Colloid Interface Sci 1999;4:283.
[8] Mehta A, Needs RJ, Thouless DJ. Europhys Lett 1991;14:113.
[9] Helfand E, Pearson DS. J Chem Phys 1983;79:2054.
[10] Mavrantzas VG, Öttinger HC. Thermodynamically founded atomistic Monte Carlo for nonequilibrium systems, Preprint, 2000.
[11] Mavrantzas VG, Theodorou DN. Macromolecules 1998;31:6310.
[12] Grmela M, Öttinger HC. Phys Rev E 1997;56:6620.
[13] Öttinger HC, Grmela M. Phys Rev E 1997;56:6633.
[14] Doi M, Edwards SF. The theory of polymer dynamics. Oxford: Clarendon Press, 1986.
[15] Press WH, Teukolsky SA, Vetterling WT, Flannery BP. Numerical recipes in Fortran 77. 2nd ed. Cambridge: Cambridge University Press, 1992.
[16] Flory PJ. Statistical mechanics of chain molecules. Munich: Hanser, 1989.
[17] Bird RB, Armstrong RC, Hassager O, Curtiss CF. Dynamics of polymeric liquids. 2nd ed, vol. 1 + 2. New York: Wiley, 1987.
[18] Pant PVK, Theodorou DN. Macromolecules 1995;28:7224.
[19] Porod G. Monatsh Chem 1949;80:251.
[20] Ianniruberto G, Marrucci G. J Non-Newtonian Fluid Mech 1998;79:225.
[21] Marrucci G, Ianniruberto G. J Non-Newtonian Fluid Mech 1999;82:275.
[22] Öttinger HC. J Non-Newtonian Fluid Mech 1988;89:165.
[23] Kröger M. Physica A 1998;249:332.